



## OPEN ACCESS

## EDITED BY

Chaojin Lu,  
University of Miami, United States

## REVIEWED BY

Zhehang Xu,  
PetroChina Hangzhou Research Institute of  
Geology, China  
Xixin Wang,  
Yangtze University, China

## \*CORRESPONDENCE

Feng Wu

✉ fengwu@hhu.edu.cn

Xinong Xie

✉ xnxie@cug.edu.cn

RECEIVED 26 July 2024

ACCEPTED 27 September 2024

PUBLISHED 30 October 2024

## CITATION

Chen B, Wu F, Xie X, Gao Y, Xiao W and  
Tang Z (2024) Sequence stratigraphic analysis  
of the late Permian Changhsingian platform  
marginal reef, Western Hubei, South China.  
*Front. Mar. Sci.* 11:1470867.  
doi: 10.3389/fmars.2024.1470867

## COPYRIGHT

© 2024 Chen, Wu, Xie, Gao, Xiao and Tang.  
This is an open-access article distributed under  
the terms of the [Creative Commons Attribution  
License \(CC BY\)](https://creativecommons.org/licenses/by/4.0/). The use, distribution or  
reproduction in other forums is permitted,  
provided the original author(s) and the  
copyright owner(s) are credited and that the  
original publication in this journal is cited, in  
accordance with accepted academic  
practice. No use, distribution or reproduction  
is permitted which does not comply with  
these terms.

# Sequence stratigraphic analysis of the late Permian Changhsingian platform marginal reef, Western Hubei, South China

Beichen Chen<sup>1,2</sup>, Feng Wu<sup>3\*</sup>, Xinong Xie<sup>2\*</sup>, Ya Gao<sup>4</sup>,  
Wang Xiao<sup>2</sup> and Zhiyi Tang<sup>2</sup>

<sup>1</sup>Research Institute, Shenzhen Branch of China National Offshore Oil Corporation Ltd.,  
Shenzhen, China, <sup>2</sup>College of Marine Science and Technology, China University of Geosciences,  
Wuhan, China, <sup>3</sup>College of Oceanography, Hohai University, Nanjing, China, <sup>4</sup>School of Marine  
Sciences, Sun Yat-sen University, Zhuhai, China

This study presents a comprehensive analysis of the late Permian platform marginal reefs in the Sichuan Basin, focusing on reefal lithofacies and sequence stratigraphic patterns. Field outcrop observations and rock sample analyses from the Jiantianba reef were conducted to establish an evolution model of sponge reef development and spatial distribution. Four stages of marginal carbonate platform were documented: open platform, gently sloping reef, steeply sloping reef, and reef bank system. Distinct lithofacies were identified in these stages, reflecting different depositional environments and growth rates. The gently sloping reef was composed of filled skeleton framestone, filled skeleton bafflestone, and micrite organism limestone, indicating limited reef-building capacity. In contrast, the lithofacies of steeply sloping reefs were composed of open skeleton framestone, open skeleton bafflestone, binding skeleton bafflestone, and benthic organism bindstone, indicating stronger reef-building ability. Based on depositional features and carbon isotopic trends, the reef strata were divided into two sequences. Sequence 1 corresponds to the formation of unit 1, and sequence 2 can be further divided into units 2 and 3. In unit 1, reefs developed in a relatively deeper-water setting. It was characterized by rich micrite limestone, forming a gentle margin. Unit 2 witnessed reef development in shallower waters. Early marine cementation and microbial clots were prevalent, contributing to form a steep margin. In the early stage of unit 3, reefs primarily developed in a tidal-controlled environment. Subsequently, reef strata experienced a transition to a wave-influenced environment, leading to the formation of a reef bank system. In general, sequence 1 mainly formed in a heterozoan-dominated factory, and reefs contributed to a relatively gently sloping platform margin. In contrast, sequence 2 formed in a photozoan-dominated factory, and reefs contributed to a relatively steeply sloping platform margin.

## KEYWORDS

Changhsingian formation, platform margin reef, sequence stratigraphy, sponge reefs, Sichuan Basin

# 1 Introduction

The Permian sponge reef has attracted significant attention due to its great prevalence worldwide (Senowbari-Daryan et al., 2005, 2007; Nakazawa et al., 2015). There have been many reports about the platform marginal reefs in the eastern part of the Sichuan Basin, which is situated in the northern part of the Yangtze Plate (Fan and Zhang, 1985; Rigby et al., 1989; Guo and Riding, 1992; Chen et al., 2012). Many of these reefs and their associated carbonate successions are now deeply buried in the Sichuan Basin, serving as high-quality reservoirs for petroleum resources (Li H., et al., 2015). Over 50 oil and gas fields with commercial value have been discovered in this area, such as the Puguang, Jiannan, Longgang, and Yuanba fields (Ma et al., 2006, 2014; Guo et al., 2016). After petroleum exploration for two decades, there is an increasing need for a deeper understanding of the Late Permian sponge reef lithofacies and reef internal structures as well as sequence stratigraphic evolution.

The Late Permian reefs in the Sichuan Basin are predominantly composed of various sponge genera, including Sphinctozoa and Inozoa. Periphyton, such as Archaeolithoporella and Tubiphytes, commonly develop on the exterior of sponge skeletons (Fan and Zhang, 1985). These reefs primarily manifest as platform marginal reefs, exhibiting complex internal structures (Hu et al., 2012b; Wu et al., 2012; Chen et al., 2018). Microbial binding plays a crucial role in reef formation (Guo and Riding, 1992), helping steepen the platform margin (Kenter et al., 2005). Based on seismic reflection characteristics, reefs can be categorized into steeply sloping reefs and gently sloping reefs (He et al., 2022), each with distinct development characteristics and evolution patterns (Mo et al., 2019). Traditionally, the Changhsingian Formation was divided into two complete third-order sequences (Wang et al., 2023). Recent studies have further divided the evolutionary stages of the Changhsingian Formation into three stages, based on reef-building organisms and microbial rock development (Wei et al., 2015; Yan et al., 2018). Some researchers have also integrated seismic and drilling core data to analyze reef migration patterns, leading to the division of three depositional units (Zuo et al., 2024).

Based on outcrop observation and carbon isotopic data from the Jiantianba sponge reef, this study conducted a comprehensive analysis of reefal lithofacies, internal structure, and sequence stratigraphic units. The results help us to better decipher the Late Permian platform marginal reef evolution in the Jiantianba area, which has important implications for understanding the characteristics of the development and evolution stages of platform marginal reefs elsewhere. In addition, the architectural depositional pattern of the Jiantianba reefs will provide valuable insights for oil and gas exploration by aiding in the identification of structural units of platform marginal reefs in seismic profiles. Furthermore, the development of a lithofacies classification diagram for sponge-dominated reefs will enhance the accuracy of depositional facies identification in drilling cores.

## 2 Geological background

### 2.1 Geological setting

The Kaijiang-Liangping Trough, situated in the northeastern part of the Sichuan Basin, is structurally linked to the northern part of the

Yangtze Plate (Li Q., et al., 2015). During the Early Permian, the Sichuan Basin underwent pronounced differential subsidence due to regional tensile stress, leading to the formation of numerous troughs and a distinctive pattern of ridges and depressions (Jiang et al., 2019; Mo et al., 2019). Subsequently, during the Late Permian, the Kaijiang-Liangping Trough was flooded, causing a gradual decrease in water depth from northwest to southeast (Gong et al., 2020; Deng et al., 2023). The above events facilitated the development of diverse sedimentary facies in this area (Deng et al., 2023), including open platform, reef, slope, shelve, and basin facies (Figure 1). The reefal facies predominantly developed around the trough, exhibiting a distribution pattern characterized by multiple parallel lines in the northwest direction. The notable “uplift and depression” paleogeographic pattern in the eastern Sichuan Basin significantly influenced the development and distribution of reefs during the period of the Changhsingian Formation (Ma et al., 2020).

Currently, the Changhsingian Formation in the Kaijiang-Liangping Trough is deeply buried, serving as a vital reservoir for petroleum resources. Notably, the platform marginal reefs along the Chengkou-EXi Trough have emerged at the surface, offering valuable opportunities to conduct analysis on the inner structure of platform marginal reefs. Several studies have focused on the sedimentary profiles of reefs such as the Honghua-Manyue reef (Wu et al., 2012), the Pan Long Dong reef (Hu et al., 2012a), and the Jiantianba reef (Chen et al., 2018). These studies have revealed the evolution regularities of the late Permian sponge reefs. However, further research is urgently necessary on the lithofacies of sponge-type reefs and the factors that lead to differences in sequence patterns at the margins of carbonate platforms.

### 2.2 Field outcrop profiles

The field outcrop (30.4573° N, 109.0772° E) in this study is situated in Jiantian Village, Hubei Province (Figure 2A). On the northeast side of Jiantian Village, a north-south cliff section occurs, exposing a classic reef outcrop known as the quarry profile (Figure 2B). Figure 2A presents an oblique UAV photograph covering approximately 1.2 square kilometers. This image set was taken using a drone-mounted oblique camera to capture field outcrops, with a positioning and orientating system (POS) used for data interpretation and processing. Section AB in Figure 2A represents open platform sedimentation, section BC depicts the front slope of the carbonate platform, section CD illustrates the platform margin reef complex, and section DF shows the open platform to basin slope sedimentation.

In the regional outcrop profile, the Changhsingian Formation strata with a thickness of ca. 250 meters are fully exposed. Figure 2B is an enlarged picture of the quarry section (Yin et al., 2022), offering the best observation of the reef complex at the platform margin, which is the primary focus of this study. This reefal stratum spans approximately 150 meters, exhibiting a comprehensive sequence of platform marginal reef evolution. The white dotted lines delineate the sedimentary units within the reef strata, representing their original depositional units, while the thick solid white lines highlight front-reef collapse/faulting patterns. The

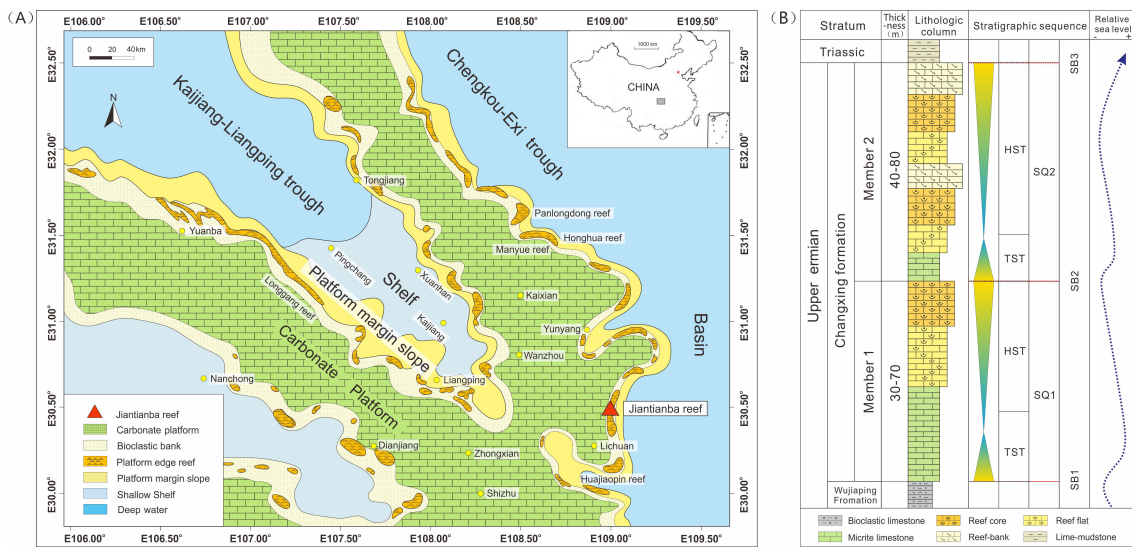


**FIGURE 1** Regional geological map. **(A)** Lithofacies paleogeography map of the Late Permian Changhsingian Formation in the Sichuan Basin; **(B)** Comprehensive schematic histogram (modified from Wang et al., 2023) of platform margin reefal strata.

three-dimensional coordinates indicate the seaward direction, facing toward the current villages' canyon (Figure 2A).

Additionally, Figure 2C exhibits carbonate platform deposition at the Changhsingian Formation's base, comprising a lower slope, upper slope, and platform top. Figure 2E shows the lower slope deposits, characterized by dark-colored limestone with high organic matter content. In contrast, Figure 2D displays the upper slope deposits, characterized by lighter-colored limestone with prominent large ripple bedding. The platform-top deposits in Figure 2C display gray-white limestone with thick to medium-layered bedding.

### 3 Materials and methods

#### 3.1 Lithofacies classification

The classification of lithological facies within reefal limestones is intricate. Traditionally, allochthonous reefal limestone types are further delineated into categories such as floatstone, rudstone, grainstone, and packstone, while autochthonous limestone comprises framestone, bafflestone, and bindstone (Dunham, 1962; Embry and Klovan, 1971; James, 1984). Two primary growth

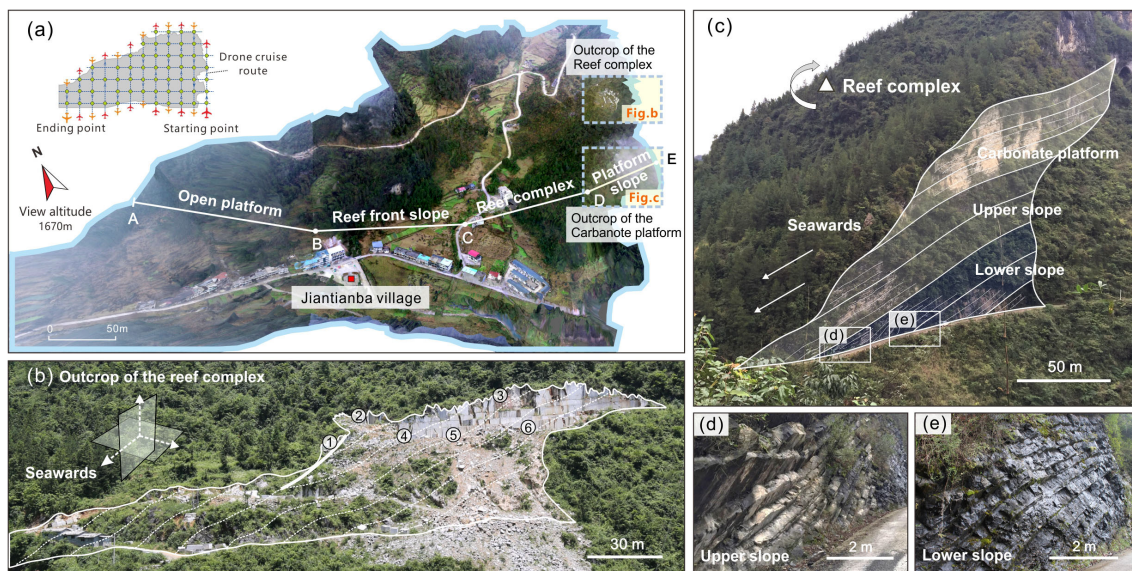


**FIGURE 2** Jiantianba reef outcrop profile. **(A)** UAV oblique photograph of Jiantianba Village (modified from Yin et al., 2022); **(B)** Reef complex outcrop profile in the quarry; **(C)** Carbonate platform slope stratigraphic profile; **(D)** Upper slope sedimentary facies; **(E)** Lower slope sedimentary facies.

patterns exist: constrictal growth and superstratal growth (Insalaco, 1998). Structural components within reefal lithofacies delineate three key end-members: matrix, skeleton, and pores/cement (Riding, 2002). Skeleton reefs are further classified into open skeleton reefs, characterized by early-stage open interspace conducive to biological crusts, early cements, intra-rock sediments, and filled skeleton reefs, where holes are filled with surface sediment during reef growth. Cemented reefs are where cement casts the reef skeleton and provides consolidation strength, imitating the function of reef-building organisms.

This study undertook a comprehensive classification of lithofacies (Scholle and Ulmer-Scholle, 2003) and depositional facies within Permian platform marginal reefs in the Sichuan Basin, aiming to refine the depositional environments and evolutionary process of sponge reefs. This helps distinguish framestone, bafflestone, and bindstone, based on the relative abundance ratios of reefal components' end-members. Additionally, the development patterns of constrictal and superstratal growth fabric between reefal skeletons are represented by open and filled skeleton reefs, respectively. In terms of reefal facies, autochthonous limestone forms the core reef facies (Chen et al., 2018), with cluster-shaped sponge skeletons occupying a significant portion of the lithological body termed the subfacies of the reef core. Furthermore, bafflestone and bindstone constitute the subfacies of the reef flat. Adjacent to the reef buildup periphery, allochthonous limestone with abundant bioclast particles and good sorting properties was identified as reef bank system sediment. Debris at the reef front slope, composed of coarse clastic particles, reefal breccia, high micrite content, and poor sorting, were designated as bioclastic flow deposits.

### 3.2 Stable-isotopes

Stable-isotope analysis ( $\delta^{18}\text{O}$  and  $\delta^{13}\text{C}$ ) was conducted on 40 samples collected from the reefal sequence outcrop from the Jiantianba village, encompassing the entire carbonate-platform marginal sequence. Each sample was collected using a dental drill, and the samples were crushed into 200 mesh powder. Approximately 80-120

$\mu\text{g}$  of powder was reacted with 105% phosphoric acid for 200-300 s at 70°C to generate  $\text{CO}_2$  before analyzing for carbon and oxygen isotopes. The generation of  $\text{CO}_2$  was performed by KIEL IV and its stable isotopes were analyzed using a MAT-253 mass spectrometer at the State Key Laboratory of Geological Processes and Mineral Resources, China University of Geosciences, Wuhan. The results are displayed in Table 1, and they are reported as permille (‰) relative to the Vienna Pee Dee belemnite (V-PDB) standard. The analytical precision for both the  $\delta^{13}\text{C}$  and  $\delta^{18}\text{O}$  values is better than  $\pm 0.1\text{‰}$ .

## 4 Results and interpretation

### 4.1 Depositional architecture

By integrating rock sample analysis and biological fossil identification, a depositional model for the Jiantianba reef was established (Figure 3G) (Chen et al., 2018). This section represents a platform-marginal reef complex, and the depositional evolution processes are divided into four stages: open platform, gently sloping reef, steeply sloping reef, and reef bank system. This classification scheme considers the external morphology of platform-marginal reefs as well as the depositional environment (Read, 1985; Reijmer, 2021). The gently sloping reef is characterized by a broad margin width and a relatively flat slope, without a significant topographic high. In contrast, the steeply sloping reef is characterized by narrower platform widths and steeper slopes, accompanied by a noticeable topographic high.

The open platform is relatively flat and is composed of massive limestone. The abundance of reef-building organisms is low, which suggests a deep-water environment. The gently sloping reef exhibits geomorphological characteristics akin to carbonate ramps, characterized by a reef core flanked by reef flats. In the reef core (Figure 3F), large clusters of sponge skeleton are prevalent, while small lodging sponge bafflestone occurs in the reef flat, displaying an interbedded pattern alongside bioclastic limestone (Figure 3F). In contrast, steeply sloping reefs display a notable topographic high at

TABLE 1 Samples location and isotope compositions (oxygen and carbon) of Limestone.

Sample	$\delta^{13}\text{C}\text{‰}$ (-VPDB)	$\delta^{18}\text{O}\text{‰}$ (-VPDB)	Sedimentary facies	Lithofacies
1	3.5	-7.3	Reef front slope	Micrite limestone
2	3.6	-8.3	Reef front slope	Micrite limestone
3	3.5	-6.3	Restricted lagoon	Bioclastic limestone
4	3.5	-6.9	Restricted lagoon	Bioclastic limestone
5	3.9	-8.0	Reef bank system	Bioclastic shell limestone bindstone
6	3.9	-8.7	Reef bank system	Bioclastic shell limestone
7	3.7	-8.5	Reef bank system	Bioclastic shell limestone
8	3.8	-8.5	Reef bank system	Bioclastic shell limestone
9	3.7	-8.3	Steeply sloping reef	Benthic organisms bindstone

(Continued)

TABLE 1 Continued

Sample	$\delta^{13}\text{C}\text{‰}$ (-VPDB)	$\delta^{18}\text{O}\text{‰}$ (-VPDB)	Sedimentary facies	Lithofacies
10	3.5	-8.8	Steeply sloping reef	Benthic organisms bindstone
11	3.4	-8.6	Steeply sloping reef	Benthic organisms bindstone
12	3.4	-8.9	Steeply sloping reef	Binding skeleton baffestone
13	3.7	-8.3	Steeply sloping reef	Binding skeleton baffestone
14	3.7	-8.1	Steeply sloping reef	Binding skeleton baffestone
15	3.9	-8.5	Steeply sloping reef	Clotted skeleton framestone
16	3.9	-8.6	Steeply sloping reef	Clotted skeleton framestone
17	4.0	-8.2	Steeply sloping reef	Clotted skeleton framestone
18	4.2	-7.9	Steeply sloping reef	Clotted skeleton framestone
19	4.2	-8.0	Steeply sloping reef	Open skeleton framestone
20	4.2	-8.5	Steeply sloping reef	Open skeleton framestone
21	4.4	-8.3	Steeply sloping reef	Open skeleton framestone
22	4.8	-7.4	Gently sloping reef	Dolomitic limestone
23	4.3	-7.1	Gently sloping reef	Dolomitic limestone
24	3.5	-8.0	Gently sloping reef	Filled skeleton baffestone
25	3.6	-8.1	Gently sloping reef	Filled skeleton baffestone
26	4.0	-8.5	Gently sloping reef	Filled skeleton baffestone
27	4.1	-8.4	Gently sloping reef	Filled skeleton framestone
28	4.0	-7.8	Gently sloping reef	Filled skeleton framestone
29	4.1	-7.6	Gently sloping reef	Filled skeleton framestone
30	3.9	-8.3	Gently sloping reef	Filled skeleton framestone
31	4.1	-8.0	Gently sloping reef	Filled skeleton framestone
32	4.1	-8.2	Gently sloping reef	Filled skeleton framestone
33	3.9	-8.1	Open platform	Micrite organism limestone.
34	3.7	-8.1	Open platform	Micrite organism limestone.
35	3.3	-8.2	Open platform	Micrite organism limestone.
36	3.2	-8.8	Open platform	Micrite organism limestone
37	3.4	-4.1	Platform slope	Lime-mudstone.
38	3.7	-3.7	Platform slope	Lime-mudstone.
39	2.6	-3.6	Platform slope	Lime-mudstone
40	2.3	-4.8	Platform slope	Lime-mudstone

the platform margin. Figure 3E illustrates the reef core of a steeply sloping reef, indicating microbial bonding processes. Specifically, (a) represents baffestone areas where sponges and bryozoans flourish, while (b) denotes sponge skeleton framestone condensed into blocks by microbials. Figure 3D shows reef flat deposits atop the steeply slope reef core. A micro-sequence of reef evolution includes (a) framestone comprised of large sponges, (b) baffestone composed of small sponges and bryozoans, (c) cement rock formed

through the binding action of red algae and microbials, and (d) lime-mudstone enriched with small organisms.

Above the steeply sloping reef formation, a set of reef-flat deposits mainly consists of the sponge baffestone and bindstone. Bioclastic shoals are distributed on the flank of the reef, and small lagoon facies occur. Reef front collapse deposits and reefal breccias in the slope were covered by a set of shallow-water limestone. Restricted lagoon facies (Figure 3C) is composed of the

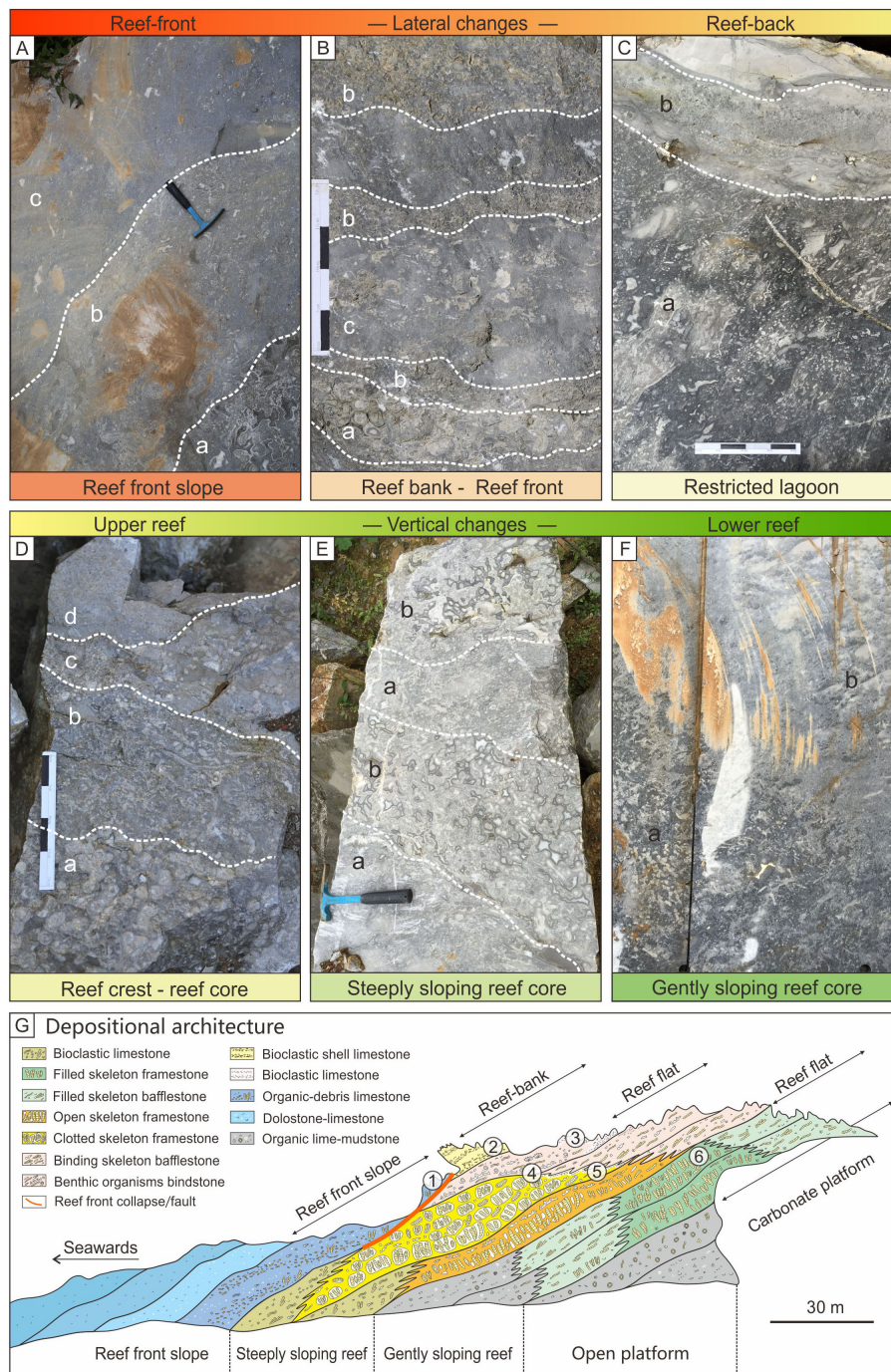


FIGURE 3

Lithofacies photos of field sections and sedimentary facies model. (A) Reef front slope: (a) eroded reef skeletal debris; (b) rudstone with coarse-grained bioclasts, (c) floatstone with a mixture of coarse clastic particles; (B) Reefal debris flow deposits: (a) bafflestone with sponge wrapped by red algae laminae; (b) rudstone dominated by coarse clastic particles, (c) floatstone with micritic limestone; (C) Restricted lagoon: (a) micrite limestone rich in small sponge organisms and (b) restricted lagoon sediments with small shells; (D) Reef crest and reef core: (a) framestone comprised of large sponges, (b) bafflestone composed of small sponges and bryozoans, (c) cement rock formed through the binding action of red algae and microbials, and (d) lime-mudstone enriched with small organisms; (E) Steeply sloping reef core: (a) bafflestone with large sponges, (b) sponge skeleton framestone condensed into blocks by microbials; (F) Gently sloping reef core: (a) large clusters of sponge skeleton, (b) interbedded pattern of bioclastic limestone and bafflestone; (G) Depositional architecture model of platform margin reef. Numbers in the circles indicate the location where the pictures above were taken.

following deposits: (a) micrite limestone rich in small sponge organisms and (b) restricted lagoon sediments with a single type of small shells. Reefal debris flow deposits (Figure 3B) are composed of the following sediments: (a) bafflestone with

sponge wrapped by red algae laminae; (b) rudstone dominated by coarse clastic particles; and (c) floatstone with micritic limestone and coarse bioclastic particles. Bioclastic deposits (Figure 3A) in the reef front slope are composed of (a) eroded

reef skeletal debris; (b) rudstone with a large amount of coarse-grained bioclasts; and (c) floatstone with a mixture of coarse clastic particles and fine-grained bioclastic limestone.

## 4.2 Reefal lithological facies

There have been reports highlighting the distinction between steeply sloping and gently sloping carbonate platform margins, based on the differences in seismic characteristics observed on either side of the Kaijiang-Liangping Trough (Wu S., et al., 2019; Mo et al., 2019). The gently sloping platform exhibits a larger marginal width and a relatively flat slope, without a significant topographic high. In contrast, steeply sloping platform margins are characterized by smaller platform widths and steeper slopes, accompanied by a noticeable topographic high. While some researchers have classified the carbonate platform margins, it is still not clear which specific reef types contribute to forming the steep or gentle platform slope. This study provides a detailed description of the lithofacies corresponding to a gently sloping platform and a steeply sloping platform (Figures 4A–J), and attempts to differentiate them in detail from the genetic mechanism.

The open platform facies is mainly composed of mudstone (Figure 4A). Overall, the color of this facies is darker and the mud content is higher. Crinoid stems develop at the bottom and contain more muddy strips. The top section is dominated by micrite limestone, with small plankton fossils such as charophytes and foraminifera. A gently sloping reef can be divided into reef core and reef flat facies. Reef core facies is mainly composed of filled skeleton sponge framestone (Figure 4B). Long strips of sponge (sphinctozoan) fossils occur, and their body cavities remain intact under the filling of micrite limestone. Reef flat facies is composed of filled sponge bafflestone (Figure 4C). The sponges are shown lying on the ground and are filled with lime mudstone. Similarly, a steeply sloping reef can also be divided into reef core and reef flat facies. Moreover, the reef core facies can be subdivided into two different lithofacies. The lower part of reef core facies is mainly composed of open skeleton framestone (Figure 4D). The sponge skeleton is wrapped by red algae laminae (*Archaeolithoporella*) and solidified by early marine cement. The sponge skeletons are in contact with each other, and the interspaces are later filled by sparry calcite cement. The upper part of reef core facies is composed of clotted skeleton framestone (Figure 4E). Smaller individual sponges are condensed into clumps by microbial influence. Early marine cement develops outside the clumps, and the interspaces are filled by sparry calcite cement, forming white diamond-shaped patches. Clotted skeleton framestone, eroded by strong hydrodynamic forces, also occurs (Figure 4F). Yellowish-gray argillaceous sediments filled the skeleton interspace. The growth sequence in reef limestone is characterized by sponge growth, red algae encrustation, microbial condensation, and early marine cementation.

The reef flat facies is mainly composed of skeletal bafflestone and bindstone. The skeletal bafflestone is composed of lodging sponges, encrusted red algae, and biological limestone (Figure 4G). A stromatactis structure occurs in this lithofacies. Skeletal bindstone is composed of micrite limestone rich in benthic

organisms (Figure 4H). Individual organisms are well preserved and are generally wrapped by lamellar red algae or condensed by microbial action. The reef bank system consists of reefal debris limestone and bioclastic shoal. The bioclastic shoal facies is dominated by shell sections of 1–2 cm in size and bright crystal cement (Figure 4I). Bioclastic breccia occurs below the reef complex (Figure 4J), which is mainly micritic limestone and contains a large amount of breccia and sponge fragments.

## 4.3 Lithofacies classification

Based on variations in lithofacies within the reef complex, distinct structural units in the platform marginal reef outcrops were identified. Notably, the geomorphological features of the platform edge are intricately linked to the gently sloping reef and steeply sloping reef types. Both types of reefs can be further subdivided into reef core and reef flat subfacies. However, notable differences exist in their lithofacies, representing distinct depositional environments, hydrodynamic strengths, and reefal construction rates. Hence, a detailed differentiation of reefal lithofacies (Figure 5) is crucial for advancing the study of regional reefs.

The lithofacies of the gently sloping reef typically exhibits characteristics of constrictal growth fabric and can be primarily categorized into three types: filled skeleton framestone, filled skeleton bafflestone, and micritic limestone. The filled skeleton framestone is characterized by a primary skeleton of sponge growth anchored within soft gray muddy sediments. The micrite limestone with planktonic organisms and charophytes filled the gap between the sponge frameworks. The filled skeleton bafflestone contains interbedded small sponges and bioclasts. Small and lying sponges acted like fences that blocked the bioclastic sediments. This lithological combination formed in multi-stage rapid deposition processes. The mudstone is composed of abundant planktonic foraminifera, charophytes, and other small organisms. This type exhibits locally high carbonate mud content and is widely distributed across the carbonate platform. In general, the sedimentation rate of the gently sloping reef is relatively high. Reef-building organisms are swiftly buried during the depositional process. The sponge skeleton could quickly fix large amounts of loose sediment, forming a slightly raised mound. As a result, the gently sloping reef did not produce significant elevation at the platform margin.

The lithofacies of a steeply sloping reef typically exhibit characteristics of superstratal growth fabric and can be primarily categorized into four types: open skeleton framestone, clotted skeleton framestone, open skeleton bafflestone, and benthic organism bindstone. The sponge skeletons in the open skeleton framestone are encrusted by lamellar red algae and tubiphytes and subsequently by marine cement. The interspace of the skeleton is also filled by sparry calcite. The characteristic of clotted skeleton framestone is that microbials were involved in the reef construction. Microbial deposits contain non-laminated clotted fabric. Microbial deposits helped bind the sponge skeleton, which was subsequently encrusted by marine cement. Open skeleton bafflestone is

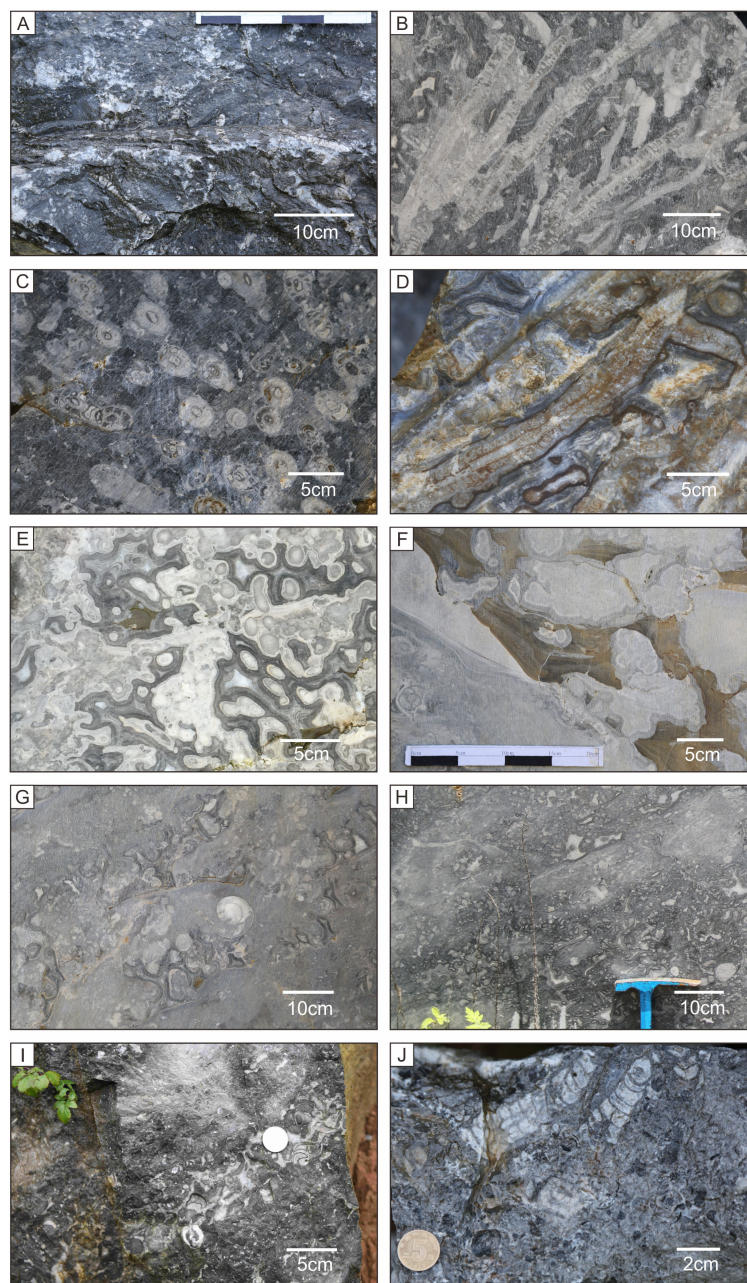


**FIGURE 4**

Photographs of typical lithofacies in reef outcrop. **(1)** Mudstone: muddy strips develop in the limestone, and more fossilized crinoid stems can be observed; **(2)** filled skeleton sponge framestone: large sponges develop into elongated shapes, the individual length can reach more than 1 m, and the body cavity remains intact. **(3)** Filled sponge bafflestone: the image shows a cross-section of a sponge. The spaces between the sponges are made of dark bioclastic limestone; **(4)** open skeleton framestone: the structure inside the body cavity of sponges (sphinctozoan) can be clearly seen. The skeletons are in contact with each other and wrapped by early marine cement. The interspace is filled with sprite calcite. **(5)** Clotted skeleton framestone: the picture shows a cross-section of sponges, which are wrapped by microbial and condensed into a clump. The gray-black lamina on the outside of the clump is early marine cement and is finally filled with diamond-shaped sparkling calcite. **(6)** Eroded skeleton framestone: reef skeleton was eroded by strong hydrodynamic events, and the interspaces were filled with gray-yellow argillaceous limestone; **(7)** skeletal bafflestone: a typical stromatactis structure developed. Lodging sponges are clotted together by microbial action, and bioclastic limestone contains nautilus; **(8)** skeletal bindstone: rich in a large number of benthic organisms, various types of small-size sponges developed, and lamellar red algae and microbial play a binding role; **(9)** bioclastic limestone: light gray bioclastic limestone interbedded with dark gray shell-rich sprite-cemented limestone; **(10)** rudstone: contains sponge fragments and biogenic breccias.

composed of interbedded small fallen sponge limestone and bioclasts. Sponges are encrusted by lamellar red algae and early marine cement. It also contains large swimming organisms such as nautilus. A stromatactis structure formed by sponges and microbial

action also occurs. Benthic organism bindstone encompasses diverse benthic organisms, displaying well-preserved individual fossils and widespread development of lamellar red algae and microbial adhesion. In general, the steeply sloping reef exhibits a

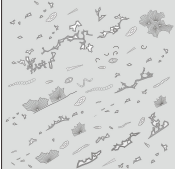
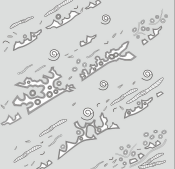
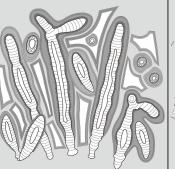
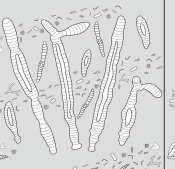
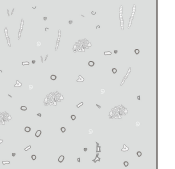
Steeply sloping reef lithofacies				Gently sloping reef lithofacies		
Non-skeleton	Skeleton-fixation	Skeleton-supporting		Skeleton-fixation		Non-skeleton
By organism which encrust and bind the deposits	By laminar algae and marine cement to encrust sponge which act as barriers; Matrix mainly consist of calcite cement	By microbes and marine cement to clot the sponge as clumpy structure; Matrix mainly consist of calcite cement	By laminar algae and marine cement to encrust sponge as rigid framework; Matrix mainly consist of calcite cement	Sponge act as skeleton fixation; Matrix consist of bioclastic limestone	Sponge act as fenestrated barriers; Matrix consist of bioclastic limestone	By organism and suspended deposits
Benthic organism bindstone	Binding skeleton bafflestone	Clotted skeleton framestone	Open skeleton framestone	Filled skeleton framestone	Filled skeleton bafflestone	Micrite organism limestone
						

FIGURE 5

Lithofacies classification diagram of sponge reefs on the margin of the Permian platform. Based on the morphology outline, the reef types can be mainly divided into two types, i.e., gently sloping type reef and steeply sloping type reef, which can be further subdivided into 7 lithofacies: benthic organism bindstone, binding skeleton bafflestone, clotted skeleton framestone, open skeleton framestone, filled skeleton framestone, filled skeleton bafflestone, and micrite organism limestone.

more convex morphology. The attachment of organisms, development of microbial action, and growth of marine cement collectively provide a hard encrustation for the reef skeleton.

#### 4.4 Stable-isotope analyses

The Jiantianba reef shows various types of diagenetic alterations, primarily including early marine cementation, deep-burial cementation, and dolomitization (Liu and Rigby, 1992). The carbon isotope composition of bulk samples with high carbonate content usually does not change significantly due to diagenesis because the carbon reservoir of the rock far exceeds the amount of carbon dissolved in diagenetic fluids (Marshall, 1992; Luo et al., 2011). Carbon and oxygen isotope analyses of Permian brachiopod fossils suggest that the  $\delta^{13}\text{C}$  values of Permian seawater during sedimentation ranged between 2.5‰ and 5.5‰ (Veizer et al., 1986). A comprehensive analysis of multiple profiles from South China indicates that the  $\delta^{13}\text{C}$  values of the Changhsingian strata averaged 2‰ in the earliest stages, while the subsequent strata were characterized by a plateau with an average of 4‰, followed by a sharp negative excursion near the Triassic boundary (Tian and Zeng, 1995; Shen et al., 2019).

Stable isotope analysis was conducted on 40 samples (Table 1) spanning the Jiantianba reef sequence, ranging from deep-water lower slope to wave-dominant reef-bank deposits. The selected samples exhibit relatively concentrated values, with  $\delta^{13}\text{C}$  ranging between 2.3‰ and 4.8‰ and  $\delta^{18}\text{O}$  ranging from -8.9‰ to -3.6‰. Specifically, the average  $\delta^{13}\text{C}$  value in the platform slope deposits is approximately 3.0‰, while the average in the open platform deposits is approximately 3.5‰. The  $\delta^{13}\text{C}$  values in the gently sloping reef deposits, steeply sloping reef deposits, and reef-front slope deposits display an average of approximately 4.1‰, 3.9‰, and 3.7‰, respectively. Among all 40 samples, the values of  $\delta^{18}\text{O}$  do

not show a specific regular change trend. However, there is a significant difference between the two sets of data. The  $\delta^{18}\text{O}$  value of the samples located in the deepwater platform slope is -4.0‰, and the other  $\delta^{18}\text{O}$  value of the samples is -8.1‰ on average.

The  $\delta^{13}\text{C}$  in the platform slope deposits exhibits lower values, ranging from 2.3‰ to 3.7‰. The average  $\delta^{13}\text{C}$  value of the lower slope deposits is 2.5‰. The average  $\delta^{13}\text{C}$  value of the upper slope deposits is 3.6‰. The average  $\delta^{18}\text{O}$  value of the platform slope deposits is -4.0‰.

The open carbonate platform deposits are characterized by moderate  $\delta^{13}\text{C}$  values ranging from 3.2‰ to 3.9‰. The  $\delta^{13}\text{C}$  values show a slightly increasing trend from bottom to top, with an average of 3.5‰, similar to the values in the upper-slope deposits. Conversely, the  $\delta^{18}\text{O}$  values of the open carbonate platform deposits average -8.3‰, significantly different from those of the slope deposits.

The gently sloping reef samples are characterized by relatively higher  $\delta^{13}\text{C}$  values ranging from 3.5‰ to 4.8‰. In this section, the  $\delta^{13}\text{C}$  values show a gradual decrease from bottom to top. At the top of this section, it reaches approximately 4.6‰. The average  $\delta^{18}\text{O}$  value of the gently sloping reef deposits is -7.9‰.

The steeply sloping reef deposits are characterized by slightly higher  $\delta^{13}\text{C}$  values ranging from 3.4‰ to 4.4‰. In this unit, there is a gradual decreasing trend in  $\delta^{13}\text{C}$  values from bottom to top. The average  $\delta^{13}\text{C}$  value is approximately 4.1‰ in the framestone, and approximately 3.6‰ in the bafflestone and bindstone. The average  $\delta^{18}\text{O}$  value of the steeply sloping reef deposits is -8.4‰, which is higher than that of the gently sloping reef deposits.

The reef bank sediments and reef front slope deposits are characterized by lower  $\delta^{13}\text{C}$  values ranging from 3.5‰ to 3.9‰. The average  $\delta^{13}\text{C}$  value of the reef bank, restricted lagoon, and front reef slope sediments is approximately 3.8‰, 3.5‰, and 3.5‰, respectively. The average  $\delta^{18}\text{O}$  value of the lagoon sediments is -6.6‰, different from the other samples from reef bank sediments.

## 5 Discussion

### 5.1 Division and comparison of stratigraphic sequence

Based on the above analysis, the platform margin reef strata can be divided into sequence 1 and sequence 2. Sequence 1 corresponds to the formation of Unit 1, and Sequence 2 can be further divided into Units 2 and 3. A transgressive systems tract (TST) and highstand systems tract (HST) were identified within each unit (Figure 6).

Unit 1 has an overall thickness of approximately 50 m. The TST is primarily composed of open-platform sediments with few reef-building organisms and is characterized by a low sedimentation rate. The  $\delta^{13}\text{C}$  values are notably low, with an average value of 3.5‰. Generally, the  $\delta^{13}\text{C}$  values of carbonate sediments tend to increase in response to the shallowing process, when the sea level declines (Swart, 2008). However, a notable negative shift in carbon isotopes occurs at the top of Sequence Unit 1, corresponding to the unconformity interface. This shift is presumably attributed to diagenesis influenced by meteoric water. The HST comprises gently sloping reef sediments, showing a higher accumulation rate and larger thickness. The  $\delta^{13}\text{C}$  values with an upward decrease indicate that the environment gradually shallowed. Sponge abundance increases from bottom to top, with large sponge clusters in the reef core and laying sponge bafflestone on the

flank. A thin sedimentary exposure surface occurs with local dolomitization and carbon excursions. This surface can be a sequence boundary (Mitchell et al., 1996), marking the end of Sequence Unit 1.

Sequence 2 is approximately 80 m thick. The lower part of the stratum is divided into Unit 2, and the upper part is divided into Unit 3. The thickness of unit 2 is approximately 40 m. The TST is thin, and it mainly consists of mudstone, indicative of rapid inundation after a brief exposure event. Above the mudstone, sponges developed, and reef-building organisms became more abundant. The HST comprises steeply sloping reef sediments, and it is characterized by a high sedimentation rate and significant microbial condensation in the reef core. Open skeleton limestone and clotted skeleton limestone dominate the lithofacies, showing a rigid skeleton structure.  $\delta^{13}\text{C}$  in this sequence exhibits a slight negative shift from bottom to top. Such a decline in  $\delta^{13}\text{C}$  hints at increased meteoric influence (Groucke et al., 1999). A significant erosive depositional event that occurred at the top of the reef core sequence supports the meteoric influence hypothesis. There are significant differences above and below the exposure surface, including the type of sedimentary facies, the abundance of sponge organisms, and the degree of microbial participation in reef building.

Unit 3 in Sequence 2 is approximately 40 m thick. The typical cluster-sponge reef core facies in the outcrop is absent. The TST is relatively thin and it is composed of reef flat facies with rich nautilus and other swimming organisms, suggesting a relatively deep-water

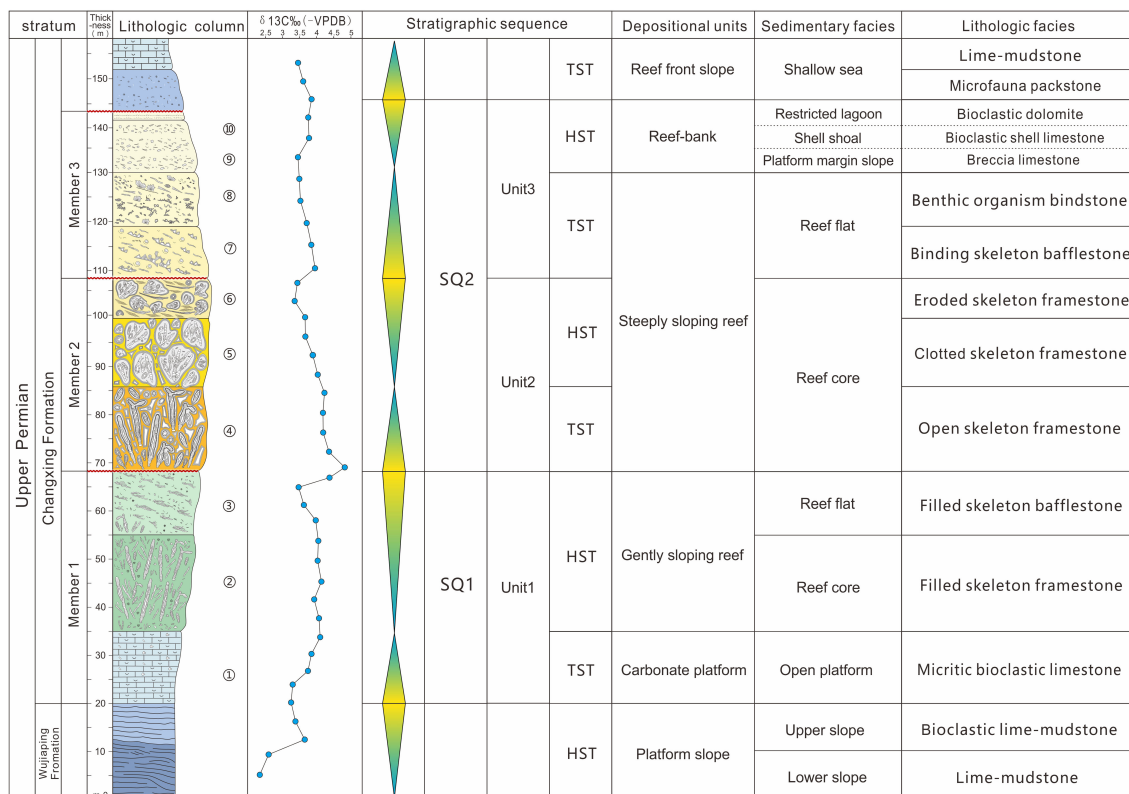


FIGURE 6 Comprehensive histogram of the Jiantianba reef. The spatial distribution characteristics of lithofacies can be found in Figure 3. The numbers in the lithologic column correspond to the photo serial numbers in Figure 4. Specific lithofacies types have a good correlation with the sequence units of reef development.

environment. In the early HST, bindstone dominates the reef flat sediments, with abundant lamellar red algae, benthic species, and well-preserved small-size sponges in lime mudstone. This reflects a shallow-water supratidal environment with low hydrodynamic conditions. In the HST, a wave-dominant reef-bank system develops. Bioclastic limestone in the top portion of the reef complex suggests a shallow shoal and lagoon environment. In general, unit 3 mainly reflects a relatively shallow water environment influenced by tides or waves.

The evolutionary pattern of the sequence stratigraphy in Jiantianba shows significant similarities to other platform marginal reefs in the region (Figure 1). The Honghua-Manyue reefs, located northwest of the Jiantianba reefs, exhibit a developmental and evolutionary process that can be divided into four depositional cycles (Wu et al., 2012). In the first and second cycles, the lithology is primarily composed of micrite sediments, with a large number of vertically oriented sphinctozoan sponges. In the third and fourth cycles, the abundance and diversity of organisms increase significantly, with lamellar red algae and microbial communities (blue-green algae) binding sponges to form framestone. Outcrop profiles reveal laminations formed by red algae encrusts and early marine cement. The Manyue reef developed on the lower part of the platform-margin slope and lacks the bioclastic banks. The Panlongdong reefs, also located northwest of Jiantianba, show a complete evolutionary process of sponge reefs in Sequence Unit 1 (Hu et al., 2012a), with framestone characteristics consistent with the reef core facies of Unit 2 in the Jiantianba reefs. The bioclastic bank and breccia developed at the top of Sequence 1 in Panlongdong reefs. They are also present in Unit 3 of the Jiantianba reefs. It is worth noting that asphalt was observed within the open skeleton lithofacies in the field outcrop sections of the Jiantianba and Panlongdong reefs, which suggests that they could serve as high-quality oil and gas reservoirs in the geological history.

## 5.2 Influence of relative sea-level changes

Relative sea level changes can significantly influence reef development (Eberli et al., 2001; Schlager, 2003; Betzler et al., 2013; Wu, F., 2019). Reef-building organisms generally thrive in shallower waters so fluctuations in sea level directly affect the vertical and horizontal distribution patterns of reef growth. The Permian marine environment differed significantly from modern oceans. The primary builders of platform marginal reefs during this period were sponges and red algae. By using a comprehensive method, we analyzed the influence of relative sea-level changes on the evolution of platform marginal sponge reefs.

During the TST in Unit 1, the carbonate platform is predominantly composed of micritic limestone with minimal skeletal debris, marked by the occasional presence of crinoid stems. This stage is characterized by high lime mud content and horizontal bedding, indicative of high relative sea levels and weak hydrodynamic conditions. During the HST, sea-level declines caused water depths suitable for sponge development. However, the sponge skeleton interspaces are filled with micritic limestone, displaying a constrictal growth pattern. Weak hydrodynamic conditions persisted, and the

micrite matrix contained more plankton. Generally, Unit 1 formed in a relatively deeper environment.

The period of TST in Unit 2 is short, forming thinner strata characterized by mudstone with small sponges, reflecting the regrowth of a biological reef after a short exposure period. In the early HST, the relative sea level fell slowly. The reef developed near the oceanic euphotic zone, leading to the large-scale proliferation of sponges, bryozoans, red algae, and other organisms. In the late HST, microbial activity began to influence the sponge reef, resulting in rapid reef construction. Storm erosion of the sponge skeletons at the upper strata suggests that the reef formed a wave-resist structure. Unit 2 occurred in a shallower environment than Unit 1.

The period of TST in Unit 3 contains lodging sponges, red algae, benthic organisms, and nautilus. Microbial clotting is present in the sponge bafflestone, but the amount is significantly reduced compared to the HST of Unit 1. In the early HST of Unit 3, the relative sea level continued to diminish, supporting the growth of a diverse benthic community, including foraminifera, small gastropods, calcareous sponges, echinoderms, and bryozoans. In the late HST, bioclastic shoals and restricted lagoon deposits indicate that the reef was close to an exposed environment. Unit 3 occurred in the shallowest environment.

Overall, in the eastern Sichuan Basin, the Late Permian Changhsingian Formation recorded a long-term relative sea level decline, subdivided into three shorter-term fluctuations. An investigation of reef-dwelling brachiopods also recorded the same paleoenvironmental changes within the Changhsingian platform-margin sponge reef in Panlongdong (Tian et al., 2022). This trend favored the development of sponge-dominated platform marginal reefs. However, in the late Changhsingian Formation, a rapid sea-level rise submerged the reefs, halting their development. The ocean environment has also undergone significant changes. This might be related to the mass extinction event between the Permian and Triassic periods.

## 5.3 Types of carbonate factory

The reef-building organisms in the Jiantianba reef complex are mainly sponges. However, there are significant differences in the characteristics of carbonates within Sequences 1 and 2 as they had developed in different marine carbonate factories (Michel et al., 2019). In order to further analyze their development and evolutionary process, it is particularly important to understand the types of carbonate factories (Westphal et al., 2010). Two carbonate factories have been proposed, namely, photozoan and heterozoan factories (James, 1997), which are applicable to the entire Phanerozoic era. Based on the petrological characteristics of the Jiantianba reef, these two carbonate factories can be identified. A photozoan carbonate factory refers to the construction of carbonate formations in shallow and warm environments, emphasizing that the energy required for carbonate precipitation comes from photosynthesis. The calcium carbonate in the seawater was in a saturated-supersaturated state. A heterozoan carbonate factory refers to a relatively deeper water environment in which the micrite content is high and the matrix contains planktonic

foraminifera. There are fewer species, mainly non-phototrophic heterotrophs, and the calcium carbonate in the seawater was in an undersaturated state.

The lower part of Unit 1 was mainly formed in a heterozoan-dominated carbonate factory. It occurred in the stage with the deepest relative sea level. In the TST stage, characterized by high sea levels and weak hydrodynamic conditions, the carbonate platform was mainly composed of mudstone with fewer reef builders. The subsequent HST stage of SQ1 experienced a rapid sea level decline, which was suitable for sponge reef development. This development pattern resembles James' thermocline slope model, with the SQ1 "reef core" corresponding to the "bryozoan-skeletal limestone" part of that model. Additionally, the mudstone filled between the sponge skeletons in SQ1, indicating the lack of typical phototrophic organism species. Here, wackestone contains abundant planktonic foraminifera and charophytes, suggesting a heterozoan carbonate factory. In the first stage, the shape of the reef is relatively gentle, and its geomorphological outline can be well compared with the seismic profile pattern, which is considered to be gently sloping reef strata around the Kaijiang-Liangping trough (Zuo et al., 2024).

Unit 2 was mainly formed in a photozoan carbonate factory. It occurred in a relatively shallower environment. The reef developed near the euphotic zone, leading to the extensive growth of sponges, bryozoans, red algae, and other organisms. Towards the late period of Unit 2, the reef skeletons were generally clotted into clumps, and most of the thrombolites were caused by microbial processes (Guo and Riding, 1992). These microbial rocks are commonly found in nutrient-rich ocean habitats (Shen et al., 2005; Che et al., 2014). Observations of the sponge skeleton at the top of Unit 2, affected by significant erosion, suggest that the reef complex could withstand the influence of strong water movement. The binding effect of lamellar red algae, marine cement, and microbial processes helped the sponge reef form a wave-resistant structure similar to modern coral colonies (KieSSLing et al., 2002). During this stage, the reef developed in a photozoan carbonate factory, characterized by the

round arch shape in the reef core area, contributing to the formation of a steeply sloping reef. The geomorphological feature is comparable with that of the steeply sloping reef strata around the Kaijiang-Liangping trough (Zuo et al., 2024).

Unit 3 was mainly formed in a photozoan-dominated carbonate factory (KieSSLing et al., 2002). During the TST, reef flat facies widely developed. A significant number of lodged sponges continued to grow in situ, with the most diverse benthic communities. The content of the micrite matrix was very high. Microbial action was also evident in reef construction during this phase. The strata witnessed the development of typical stromatolite structures and porous formations, characteristic of microbial rocks (Bathurst, 1982; Bourque, 1994). These structures are characterized by irregularly shaped holes filled with late calcite cement. In the late stage of Unit 3, typical reef bank sediments occurred (Tan et al., 2020). It is speculated that this was related to the fact that the sponge-type reef had formed a hard skeleton capable of resisting strong hydrodynamic conditions.

## 5.4 Characteristics of reefal sequence pattern

In the study area, the predominant reef-building organisms are Permian sponges. Different carbonate factories result in distinct processes of reef growth. The interaction of sponges with red algae, microbials, and early marine cements varies across different marine environments, leading to significant differences in reef stratigraphic patterns. Consequently, the Jiantianba reef appears to have distinguished sequence patterns of gently sloping reef strata (Figures 7A, B) and steeply sloping reef strata (Figures 7C, D), each exhibiting unique sequence characteristics of HST and TST phases at the edge of carbonate platforms.

Heterozoan-dominated reefs formed a relatively gently sloping margin. *In situ* growth of sponges and loose micritic sediments resulted in a relatively parallel and equal-thickness growth pattern at the edge of

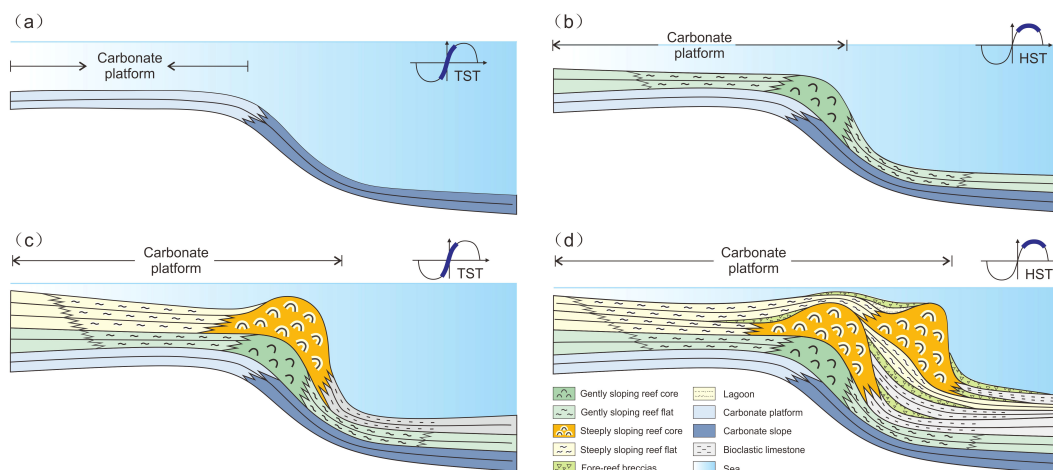


FIGURE 7

Sequence stratigraphic patterns of the heterozoan-dominated reefs and photozoan-dominated reefs. These patterns are the characteristic of (A) heterozoan-dominated reefs in the transgressive system tract; (B) heterozoan-dominated reefs in the highstand system tract; (C) photozoan-dominated reefs in the transgressive system tract; (D) photozoan-dominated reefs in the highstand system tract.

the carbonate platform. During the TST of the heterozoan-dominated reefs, the rapid rise in relative sea level triggered compensatory sedimentation and inundation of the platform, significantly impeding the growth rate of the reef formations (Figure 7A). During the HST of the heterozoan-dominated reefs, an aggradation pattern appears on the platform edge. In the beginning, the growth rate of the reef was relatively equivalent to the change rate of the accommodation space at the platform edge, leading to a parallel aggradation pattern. Subsequently, as the growth rate of the reef was slightly greater than the change rate of the accommodating space, the stratigraphic style also transitioned from the aggradation style to the progradation style, causing the carbonate platform as a whole to be in a relative expansion stage (Figure 7B).

Photozoan-dominated reefs formed a relatively steeply sloping margin. During the development of sponge reef, large calcareous algae developed in a phototrophic environment, early marine cements formed under the action of carbonate supersaturation, and clots formed under the action of microbial coagulation. These facts together led to rapid reef growth, forming a raised shape at the platform margin and making the slope steeper. During the TST, the rate of reef development aligned with the rising relative sea level. In the early stage of the TST, sponges began to aggrade at the platform's margin. However, in the later stage of TST, the growth rate of reef strata lagged behind the increase in accommodation space, causing reefs to migrate to higher positions. When the water depth increased sufficiently, reef development ceased (Figure 7C). During the HST of the photozoan-dominated reefs, the growth potential of the reef was significantly greater than the increase in accommodation space, and the reef grew rapidly. When there was insufficient accommodation, the reef complex was forced to grow toward the slope area, and the stratigraphic style exhibited a progradation pattern, causing a rapid expansion of the carbonate platform (Figure 7D).

## 6 Conclusion

1. During the Late Permian, the evolution pattern of the carbonate platform in the Sichuan Basin was significantly influenced by reef growth at the platform margin. Two types of sponge reefs, namely heterozoan-dominated reefs and photozoan-dominated reefs, were identified, each characterized by unique external forms and different lithofacies associations. The heterozoan-dominated reef is characterized by filled skeleton framestone, filled skeleton bafflestone, and micrite organism limestone lithofacies. Conversely, the photozoan-dominated reef is composed of the lithofacies of open skeleton framestone, open skeleton bafflestone, binding skeleton bafflestone, and benthic organism bindstone.
2. In Unit 1 of Sequence 1, the reef complex exhibits a gently sloping platform margin, similar to heterozoan-dominated deposits. In Unit 2 of Sequence 2, the reef complex exhibits a steeply sloping platform margin, similar to a photozoan-type carbonate factory. The involvement of red algae, marine cement, and microbials in the construction of sponge reefs contributed to the development of a robust framework critical

for reef sustainability. In the early stage of Unit 3, the reef strata displayed the features of carbonate mounds, showing a diverse array of benthic organisms and observable microbial clots. In the late stage of Unit 3, there was an emergence of a typical reef-bank system, accompanied by the development of debris flow deposits on the reef front slope.

3. Heterozoan-dominated reefs contributed to a gently sloping margin, while photozoan dominated-reefs contributed to form a relatively steeply sloping margin. Relative sea level changes were not the only factor that affected reef development. Sponges developed in different water depths, and the binding effect of microbial action and marine cements greatly changed the strength of the reef complex and therefore the morphology of the platform margin.

## Data availability statement

The original contributions presented in the study are included in the article/supplementary material. Further inquiries can be directed to the corresponding authors.

## Author contributions

BC: Writing – original draft, Writing – review & editing. FW: Writing – original draft, Writing – review & editing. XX: Writing – original draft, Writing – review & editing. YG: Writing – original draft. XW: Writing – original draft. ZT: Writing – original draft.

## Funding

The author(s) declare financial support was received for the research, authorship, and/or publication of this article. This research is funded by the National Natural Science Foundation of China (Grant No.42130408; 42106058).

## Conflict of interest

Author BC was employed by the company Shenzhen Branch of China National Offshore Oil Corporation Ltd.

The remaining authors declare that the research was conducted in the absence of any commercial or financial relationships that could be construed as a potential conflict of interest.

## Publisher's note

All claims expressed in this article are solely those of the authors and do not necessarily represent those of their affiliated organizations, or those of the publisher, the editors and the reviewers. Any product that may be evaluated in this article, or claim that may be made by its manufacturer, is not guaranteed or endorsed by the publisher.

## References

- Bathurst, R. G. C. (1982). Genesis of stromatolite cavities between submarine crusts in palaeozoic carbonate mud buildups[J]. *J. Geological Soc.* 139 (2), 165–181. doi: 10.1144/gsjgs.139.2.0165
- Betzler, C., Fürstenau, J., Lüdman, T., Hübscher, C., Lindhorst, S., Paul, A., et al. (2013). Sea-level and ocean-current control on carbonate-platform growth, maldives, indian ocean. *Basin Res.* 25, 172–196. doi: 10.1111/j.1365-2117.2012.00554.x
- Bourque, P. A., and Raymond, L. (1994). Diagenetic alteration of early marine cements of upper silurian stromatolite[J]. *Sedimentology* 41 (2), 255–269. doi: 10.1111/j.1365-3091.1994.tb01404.x
- Chen, B., Xie, X., Al-Aasm, I. S., Wu, F., and Zhou, M. (2018). Depositional architecture and facies of a complete reef complex succession: a case study of the Permian Jiantianba Reefs, Western Hubei, South China. *Minerals* 8, 533. doi: 10.3390/min8110533
- Chen, L., Lu, Y., Guo, T., Xing, F., and Jiao, Y. (2012). Seismic sedimentology study in the high-resolution sequence framework—a case study of platform margin reef-beach system of Changxing formation, Upper Permian, Yuanba Area, Northeast Sichuan Basin, China. *J. Earth Sci.* 23, 612–626. doi: 10.1007/s12583-012-0278-x
- Deng, M., Zhao, G., Lin, X., Chen, C., Li, L., and Liang, Q. (2023). Sedimentary facies, paleogeography, and depositional models of the middle-late permian in the Sichuan Basin, Southwest China. *Minerals* 13, 1406. doi: 10.3390/min13111406
- Dunham, R. J. (1962). Classification of carbonate rocks according to depositional textures. *AAPG* 1, 108–121.
- Eberli, G. P., Anselmetti, F. S., Kenter, J. A. M., Mcneil, D. F., and Melim, L. A. (2001). “Calibration of seismic sequence stratigraphy with cores and logs,” in *Subsurface geology of a prograding carbonate platform margin, great bahama bank: results of the bahamas drilling project*. Eds. R. N. Ginsburg and E. R. Warzeski (Tulsa: Society for Sedimentary Geology (SEPM)), 241–265.
- Embry, A. F., and Klovan, J. E. (1971). A late Devonian reef tract on northeastern Banks Island, NWT. *Bull. Can. petroleum geology* 19, 730–781.
- Fan, J., and Zhang, W. (1985). Sphinctozoans from late permian reefs of Lichuan, West Hubei, China. *Facies* 13, 1–43. doi: 10.1007/BF02536900
- Gong, X., Yang, W., Li, W., Zhou, X., Tang, Q., Zhang, J., et al. (2020). Characteristics and geological properties of seismic bright spots in the Permian carbonate deposit, Changshing Formation, Longgang Area, Northeast Sichuan Basin, China. *Carbonates Evaporites* 35, 1–14. doi: 10.1007/s13146-020-00631-3
- Groücke, D. R., Hesselbo, S. P., and Jenkyns, H. C. (1999). Carbon-isotope composition of Lower Cretaceous fossil wood: Ocean-atmosphere chemistry and relation to sea-level change. *Geology* 27, 155–158. doi: 10.1130/0091-7613(1999)027<0155:CICOLC>2.3.CO;2
- Guo, C., Li, G., Wei, H., Xia, F., and Xie, F. (2016). Stratigraphic architecture and platform evolution of the Changxing Formation (Upper Permian) in the Yuanba Gas Field, northeastern Sichuan Basin, China. *Arabian J. Geosciences* 9, 1–23. doi: 10.1007/s12517-016-2348-3
- Guo, L., and Riding, R. (1992). Microbial micritic carbonates in uppermost Permian reefs, Sichuan Basin, southern China: some similarities with Recent travertines. *Sedimentology* 39, 37–53. doi: 10.1111/j.1365-3091.1992.tb01022.x
- He, W., Meng, Q., Bai, X., Wang, X., Wang, Y., and Tan, W. (2022). Evolution and exploration direction of Permian-Triassic multiphase platform margin in northeast Sichuan Basin. *Acta Petroli Sin.* 43, 1201. doi: 10.7623/syxb202209001
- Hu, M., Hu, Z., Qiu, X., Zhao, E., and Wang, D. (2012a). Platform edge reef and bank structure and depositional model of Changxing formation in Panlongdong section, Xuanhan, northeastern Sichuan. *J. Earth Sci.* 23, 431–441. doi: 10.1007/s12583-012-0266-1
- Hu, M., Wei, H., Qiu, X., and Zhao, E. (2012b). Reef composition and their forming models of Changxing Formation in Jiantianba Section of Lichuan, Western Hubei. *Acta Sedimentologica Sin.* 30, 33–42.
- Insalaco, E. (1998). The descriptive nomenclature and classification of growth fabrics in fossil scleractinian reefs. *Sedimentary Geology* 118 (1-4), 159–186. doi: 10.1016/S0037-0738(98)00011-6
- James, N. P. (1984). Shallowing-upward sequences in carbonates[J]. *Facies and models (2nd edition)* 1, 213–228.
- James, N. P. (1997). “The cool-water carbonate depositional realm,” in *Cool-Water Carbonates*. Eds. N. P. James and M. J. Clarke (Society for Sedimentary Geology (SEPM) Special Publications, Society for Sedimentary Geology, SEPM, Tulsa, USA), 1–20.
- Jiang, Y., Diao, Z., and Xu, C. (2019). Characteristics and controlling factors of Permian reef beach reservoir in platform-depression margin of eastern Sichuan Basin. *Special Oil Gas Reservoirs* 27, 7–13. doi: 10.3969/j.issn.1006-6535.2020.05.002
- Kenter, J. A., Harris, P. M. M., and Della Porta, G. (2005). Steep microbial boundstone-dominated platform margins—examples and implications. *Sedimentary Geol.* 178 (1–2), 5–30. doi: 10.1016/j.sedgeo.2004.12.033
- Kiessling, W., Flügel, E., and Golonka, J. (2002). *Phanerozoic reef patterns* (SEPM Society for Sedimentary Geology).
- Li, H., Long, S., You, Y., Liu, G., and Li, X. (2015). Sequence and sedimentary features of the Changxing Fm organic reefs and their control on reservoir development in the Yuanba Gas Field, Sichuan Basin. *Natural Gas Industry B* 2, 506–514. doi: 10.1016/j.ngib.2015.12.004
- Li, Q., Miao, S., Wang, T., Jiang, Q., Wang, Z., Li, J., et al. (2015). Sedimentary filling configuration of Yangtongnan trough under the background of intracratonic rift in Later Permian, Sichuan Basin. *Earth Sci. Front.* 22, 67.
- Liu, H., and Rigby, J. K. (1992). Diagenesis of the upper permian jiantianba reef, West Hubei, China. *J. Sedimentary Res.* 62, 367–381. doi: 10.1306/D4267906-2B26-11D7-864800102C1865D
- Luo, G., Wang, Y., Yang, H., Algeo, T. J., Kump, L. R., Huang, J., et al. (2011). Stepwise and large-magnitude negative shift in  $\delta^{13}\text{C}_{\text{carb}}$  preceded the main marine mass extinction of the Permian–Triassic crisis interval. *Palaeogeography Palaeoclimatology Palaeoecol.* 299, 70–82. doi: 10.1016/j.palaeo.2010.10.035
- Ma, Y., Cai, X., and Zhao, P. (2014). Characteristics and formation mechanisms of reef-shoal carbonate reservoirs of Changxing-Feixianguan formations, Yuanba gas field. *Acta Petroli Sin.* 35, 1001. doi: 10.7623/syxb201406001
- Ma, Y., Mu, C., Guo, X., Tan, Q., and Yu, Q. (2006). Characteristic and framework of the Changxingian sedimentation in the northeastern Sichuan Basin. *Geological Rev.* 52, 25–29.
- Ma, D., Tian, J., Lin, X., Wen, L., and Xu, L. (2020). Differences and controlling factors of Changxing Formation reefs of the Permian in the Sichuan Basin. *Oil Gas Geology* 41, 1176–1187.
- Marshall, J. D. (1992). Climatic and oceanographic isotopic signals from the carbonate rock record and their preservation. *Geological magazine* 129, 143–160. doi: 10.1017/S0016756800008244
- Michel, J., Laugié, M., Pohl, A., Lanteaume, C., Masse, J. P., Donnadieu, Y., et al. (2019). Marine carbonate factories: a global model of carbonate platform distribution. *Int. J. Earth Sci.* 108, 1773–1792. doi: 10.1007/s00531-019-01742-6
- Mitchell, S. F., Paul, C. R. C., and Gale, A. S. (1996). Carbon isotopes and sequence stratigraphy. *Geological Society London Special Publications* 104, 11–24. doi: 10.1144/GSL.SP.1996.104.01.02
- Mo, W., Su, N., Wei, G., Yang, W., Liu, M., Xing, F., et al. (2019). Structural control, seismic expression, and types of reefs of rifting margins in the late Permian Changxing Age, Sichuan Basin, China. *Arabian J. Geosciences* 12, 1–13. doi: 10.1007/s12517-019-4720-6
- Nakazawa, T., Igawa, T., Ueno, K., and Fujikawa, M. (2015). Middle Permian sponge–microencruster reefal facies in the mid-Panthalassan Akiyoshi atoll carbonates: observations on a limestone slab. *Facies* 61, 1–14. doi: 10.1007/s10347-015-0443-7
- Read, J. F. (1985). Carbonate platform facies models. *AAPG Bull.* 69, 1–21. doi: 10.1306/AD461B79-16F7-11D7-8645000102C1865D
- Reijmer, J. J. G. (2021). Marine carbonate factories: Review and update. *Sedimentology* 68, 1729–1796. doi: 10.1111/sed.12878
- Riding, R. (2002). Structure and composition of organic reefs and carbonate mud mounds: concepts and categories. *Earth-Science Rev.* 58, 163–231. doi: 10.1016/S0012-8252(01)00089-7
- Rigby, J. K., Jiasong, F., and Wei, Z. (1989). Sphinctozoan sponges from the Permian reefs of South China. *J. Paleontology* 63 (4), 404–439. doi: 10.1017/S002233600001965X
- Schlager, W. (2003). Benthic carbonate factories of the Phanerozoic[J]. *Int. J. Earth Sci.* 92, 445–464.
- Scholle, P. A., and Ulmer-Scholle, D. S. (2003). *A Color Guide to the Petrography of carbonate Rocks: AAPG Memoir*, Vol. 77. 474 p.
- Senowbari-Daryan, B., Hamedani, A., and Rashidi, K. (2007). Sponges from the Permian of Hambast Mountains, south of Abadeh, central Iran. *Facies* 53, 575–614. doi: 10.1007/s10347-007-0119-z
- Senowbari-Daryan, B., Rashid, K., and Hamedani, A. (2005). Sponge assemblage from the Permian reefal limestones of Kuh-e Bagh-e Vang, Shotori Mountains (eastern Iran). *GEOLOGICA CARPATHICA-BRATISLAVA* - 56, 381.
- Shen, S., Zhang, H., Zhang, Y., Yuan, D., Chen, B., He, W., et al. (2019). Permian integrative stratigraphy and timescale of China. *Sci. China Earth Sci.* 62, 154–188. doi: 10.1007/s11430-017-9228-4
- Swart, P. K. (2008). Global synchronous changes in the carbon isotopic composition of carbonate sediments unrelated to changes in the global carbon cycle[J]. *Proc. Natl. Acad. Sci.* 105 (37), 13741–13745. doi: 10.1073/pnas.0802841105
- Tan, L., Liu, H., Tang, Y., Luo, B., Zhang, Y., Yang, Y., et al. (2020). Characteristics and mechanism of Upper Permian reef reservoirs in the eastern Longgang Area, northeastern Sichuan Basin, China. *Petroleum* 6, 130–137. doi: 10.1016/j.petlm.2019.06.008
- Tian, J. C., and Zeng, Y. F. (1995). The evolution pattern of the carbon and oxygen isotopes in the Permian marine carbonate rocks from Guizhou. *J. Chengdu Institute Technol.* 22, 78–82. doi: 10.1002/ar.25023
- Tian, X., Wang, W., Huang, Z., Zhang, Z., and Chen, D. (2022). Reef-dwelling brachiopods record paleoecological and paleoenvironmental changes within the

Changhsingian (late Permian) platform-margin sponge reef in eastern Sichuan Basin, China. *Anatomical Rec.* doi: 10.1002/ar.25023

Veizer, J., Fritz, P., and Jones, B. (1986). Geochemistry of brachiopods: oxygen and carbon isotopic records of Paleozoic oceans. *Geochimica Cosmochimica Acta* 50, 1679–1696. doi: 10.1016/0016-7037(86)90130-4

Wang, D., Liu, H., Tang, S., Bai, J., Zhou, G., and Li, Z. (2023). Sedimentary architecture and distribution of intra-platform shoal in sequence framework of Permian Changxing Formation in central Sichuan Basin, SW China. *Petroleum Explor. Dev.* 50, 346–359. doi: 10.1016/S1876-3804(23)60395-7

Wei, Y., Zhang, T., Wei, G., Yang, W., Liu, M., Liu, Z., et al. (2015). Sedimentological architecture of the late permian carbonate platform margin to the west of Chengkou-Western Hubei Oceanic trough, Sichuan, China. *Geological J. China Universities* 21, 79. doi: 10.16108/j.issn1006-7493.2014142

Westphal, H., Halfar, J., and Freiwald, A. (2010). Heterozoan carbonates in subtropical to tropical settings in the present and past. *Int. J. Earth Sci.* 99, 153–169. doi: 10.1007/s00531-010-0563-9

Wu, F., Xie, X. N., Betzler, C., Zhu, W. L., Zhu, Y. H., Guo, L. Y., et al. (2019). The impact of eustatic sea-level fluctuations, temperature variations and nutrient-level changes since the pliocene on tropical carbonate platform (Xisha islands, south china sea). *Palaeogeogr. Palaeoclimatol. Palaeoecol.* 514, 373–385. doi: 10.1016/j.palaeo.2018.10.013

Wu, L., Jiao, Y., Rong, H., Wang, R., and Li, R. (2012). Reef types and sedimentation characteristics of Changxing formation in Manyue-Honghua Section of Kaixian, Northeastern Sichuan Basin. *J. Earth Sci.* 23, 490–505. doi: 10.1007/s12583-012-0270-5

Wu, S., Wei, G., Yang, W., Duan, S., Jin, H., Xie, W., et al. (2019). Development characteristics of reefs on the platform margin of Changxing Formation in eastern Kaijiang-Liangping ocean trough and its significance for petroleum geological exploration. *China Petroleum Explor.* 24, 457. doi: 10.3969/j.issn.1672-7703.2019.04.006

Yan, Z., Xing, F., Duan, J., Hu, H., and Wu, S. (2018). Sedimentary texture and reservoir distribution of platform margin reef-flat zone in Changxing formation of Northeastern Sichuan Basin. *Xinjiang Petroleum Geology* 39, 1. doi: 10.7657/XJPG20180308

Yin, S., Zhao, L., Lin, Y., Zhu, B., Zhao, J., Cheng, L., et al. (2022). Quantitative 3-D model of carbonate reef and shoal facies based on UAV oblique photogrammetry data: A case study of the jiantanba outcrop in West Hubei, China. *Front. Earth Sci.* 10, 882499. doi: 10.3389/feart.2022.882499

Zuo, M., Wang, J., Sun, X., Hu, Z., Bai, Y., Yang, W., et al. (2024). Platform margin belt structure and sedimentation characteristics of Changxing Formation reefs on both sides of the Kaijiang-Liangping trough, eastern Sichuan Basin, China. *Open Geosciences* 16, 20220615. doi: 10.1515/geo-2022-0615